Nuclear Instruments and Methods in Physics Research A 815 (2016) 96–103

Contents lists available at ScienceDirect

Nuclear Instruments and Methods in Physics Research A

journal homepage: www.elsevier.com/locate/nima

The ^{3}He long-counter TETRA at the ALTO ISOL facility

D. Testov [a,b,*], D. Verney [a], B. Roussière [a], J. Bettane [a], F. Didierjean [c], K. Flanagan [d], S. Franchoo [a], F. Ibrahim [a], E. Kuznetsova [a], R. Li [a], B. Marsh [f], I. Matea [a], Yu. Penionzhkevich [b,e], H. Pai [g], V. Smirnov [b], E. Sokol [b], I. Stefan [a], D. Suzuki [a], J.N. Wilson [a]

[a] Institut de Physique Nucléaire, CNRS-IN2P3, Univ. Paris-Sud, Université Paris-Saclay 91406 Orsay Cedex, France
[b] Joint Institute for Nuclear Research, Joliot-Curie 6, 141980 Dubna, Moscow Region, Russia
[c] Institut Pluridisciplinaire Hubert Curien, CNRS-IN2P3, University of Strasbourg, 67037 Strasbourg cedex 2, France
[d] University of Manchester, Oxford Road, Manchester M13 9PL, United Kingdom
[e] National Research Nuclear University, Kashirskoye Shosse 31, Moscow 115409, Russia
[f] CERN, CH-1211 Geneva 23, Switzerland
[g] Institut für Kernphysik, Technische Universität Darmstadt, D-64289 Darmstadt, Germany

ARTICLE INFO

Article history:
Received 5 December 2014
Received in revised form
18 November 2015
Accepted 20 November 2015
Available online 22 January 2016

Keywords:
^{3}He counters
β-Decay
Neutron emission
Radioactive beams (RIB)

ABSTRACT

A new β-decay station (BEDO) has been installed behind the PARRNe mass separator operated on-line at the electron-driven ALTO ISOL facility. The station is equipped with a movable tape collector allowing the creation of the radioactive sources of interest at the very center of a modular detection system. The mechanical structure was designed to host various assemblies of detectors in compact geometry. We report here the first on-line use of this system equipped with the 4π ^{3}He neutron counter TETRA built at JINR Dubna associated with HPGe and plastic 4π β detectors. The single neutron detection efficiency achieved is 53(2)% measured using the ^{252}Cf source. For β-delayed neutron measurements the neutron detection efficiency was derived from the comparison of gated γ-spectra. The on-line commissioning of the TETRA setup was performed with laser-ionized gallium beams. β and neutron events were recorded as a function of time. From these data we report $P_{1n}(^{82}\mathrm{Ga})=22(2)\%$ and $T_{1/2}(^{82}\mathrm{Ga})=0.604(11)$ s in good agreement with values available in the literature. The new detection system will be used in other experiments aimed at investigations of β-decay properties of neutron-rich isotopes produced at ALTO.

1. Introduction

During the last decade beams of neutron-rich nuclei of very hard-to-reach mass regions, such as the region of ^{78}Ni, have become available [1]. To understand the role of neutron excess in the shell evolution in these regions many experimental efforts are pursued. Global properties of β-decay such as half-life ($T_{1/2}$) and probability of β-delayed neutron emission (P_n) can provide the first hints on the structure of these nuclei. In addition, β-decay properties are crucial input parameters for astrophysical models of the rapid neutron capture-process (r-process), see e.g. [2,3] and the references therein. A carefully characterized neutron detector to study the properties of exotic nuclei is, therefore, indispensable.

Neutron detection methods are based on the detection of secondary charged particles produced as a consequence of neutron interaction with a detection media – the active material of the detector. Various media can be used resulting in many possible options for a neutron detector. Since the production rate of very neutron rich isotopes can be low, high efficiency neutron detection setups are essential. ^{3}He detection media are known to provide uniformly high efficiency of neutron detection below 1 MeV(~ 40 −70%) and negligible energy threshold [4]. Since the energy spectra of β-delayed neutrons emitted by nuclei far from stability are in general not known, modern neutron detection systems should have a constant neutron efficiency within the largest possible neutron energy range. Furthermore, since the detection of neutrons is based on a capture reaction, ^{3}He detection arrays are free from cross-talks allowing the possibility for neutron multiplicity measurements. It explains the continuous success of ^{3}He counters over several decades and the recently increased interest for the measurements of very neutron-rich isotopes [5,6].

We report in this paper on the installation and commissioning of the ^{3}He neutron counter TETRA at the BEDO (BEta Decay studies at Orsay) β-decay station recently installed [8] at the PARRNe mass-separator operating on-line at the electron-driven ALTO ISOL facility. The performances and characteristics of the TETRA

* Corresponding author: Institut de Physique Nucléaire, CNRS-IN2P3, Univ. Paris-Sud, Université, Paris-Saclay 91406 Orsay Cedex, France and Joint Institute for Nuclear Research, Joliot-Curie 6, 141980 Dubna, Moscow, Region, Russia.
Tel.: +74962164843; fax: +74962128 933.
E-mail address: dumon@jinr.ru (D. Testov).

http://dx.doi.org/10.1016/j.nima.2015.11.150
0168-9002/

detector will be detailed in Section 2. In Section 3 the experimental conditions for the commissioning of the TETRA detector coupled to the BEDO station using laser-ionized radioactive Ga beams are described. Results on decay properties, $T_{1/2}$ and P_{1n}, of the chosen test case ^{82}Ga obtained within this commissioning run are presented.

2. TETRA detector for on-line measurements at ALTO.

A description of the ALTO ISOL facility can be found in [9,10]. At ALTO radioactive ion beams are available as mass-separated (with a mass resolution of $A/dA = 1500$) photo-fission fragments at the ion-source extraction energy of 30 keV. Radioactive sources of interest are created by the interception of the beam by a movable Al-coated Mylar tape. The BEDO mechanical frame was designed to host various types of detectors positioned in compact geometry around the implantation point. In its neutron detection mode the detector assembly comprises a 4π β plastic scintillator counter, a HPGe detector and 80 ^{3}He filled neutron counters. The geometrical arrangement of the detection array for the neutron detection mode, as shown in Fig. 1(a) and (b), was optimized to allow beam collection at the center of the array. The implantation point is located at the center of the 13 cm diameter cavity on a mylar tape and is surrounded by a 3 mm thick plastic scintillator (BC408) cylinder for β detection. The tape and the plastic scintillator are operated at a pressure of 10^{-5} mbar inside the beam line. The 4π β scintillator is connected to a photo-multiplier (PM) tube located at 90° by a 50 cm light guide. The beam line is surrounded by 80 ^{3}He neutron counters, arranged in a polyethylene matrix to cover a solid angle close to 4π. One tapered coaxial HPGe detector of the EUROGAM-1 type [11] placed on the beam line axis from the backward side 5 cm away from the implantation point provides ~ 0.8% of γ-efficiency for 1 MeV. The constructed matrix for ^{3}He counters has a hexagonal arrangement and is shown in Fig. 1(c). The matrix is split into two movable parts to provide an easy access to the beam line containing the plastic scintillator and the mylar tape. The neutron counters are embedded in high-density polyethylene and are arranged in four rows so that the distance between their centers is 5 cm. The 5th ring currently does not

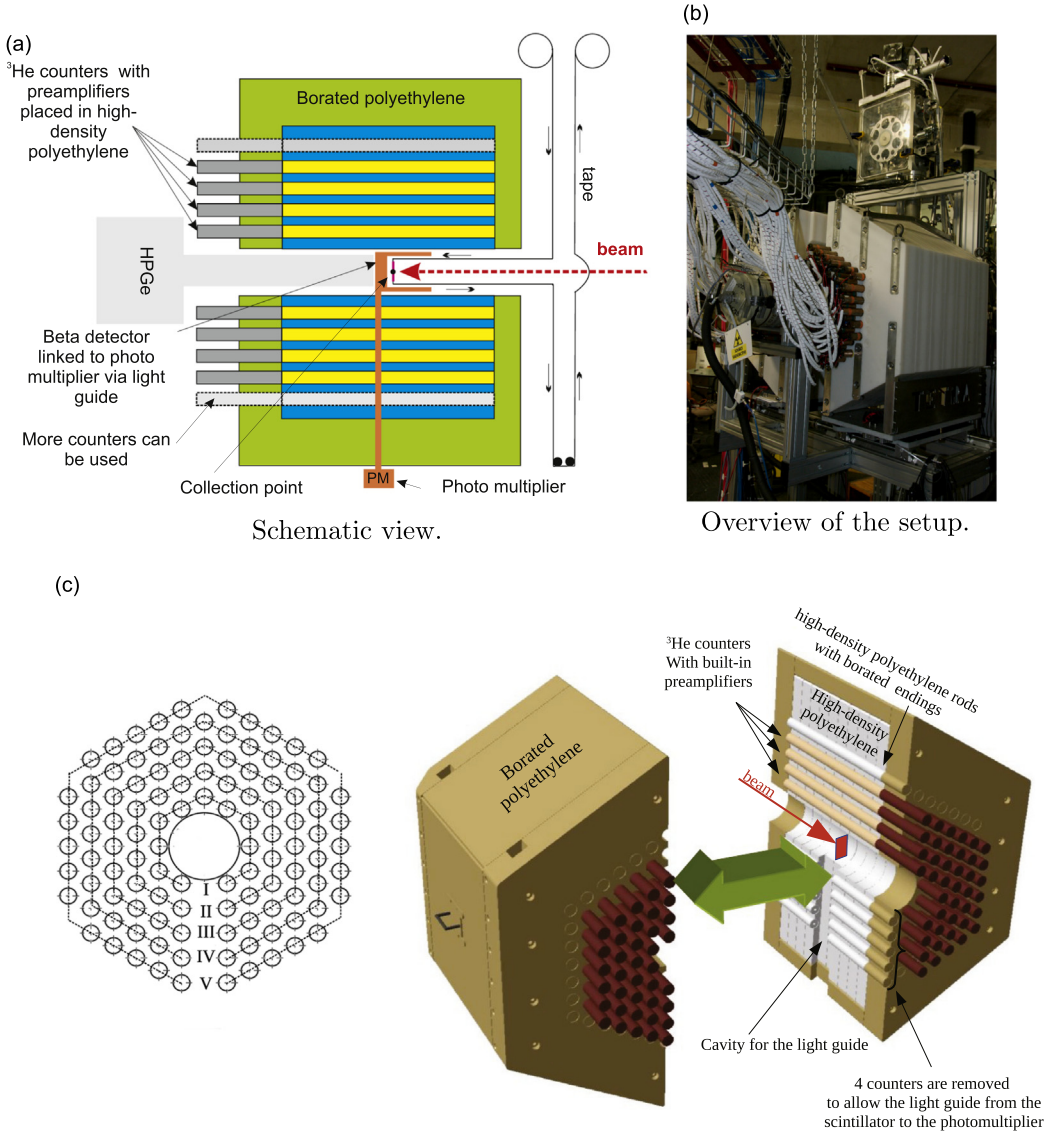

Fig. 1. *Top*: Sectional view of the detection array optimized for neutron detection, including the 4π long counter TETRA at the BEDO tape station, see text for details. *Bottom*: high-density polyethylene matrix placed inside borated 15-cm thick polyethylene frame to accommodate 80 ^{3}He counters in four rings: I (inner)—11; II—17, III—23, IV (outer)—29 counters as shown in the inset. The diameter of the center cavity is 13 cm. The 5th ring contains no counters but is filled by polyethylene rods with similar dimensions as ^{3}He counters.

contain counters but is filled by polyethylene rods made to have the dimensions of a counter as shown in Fig. 1. A layer of 15 cm thick 5% borated polyethylene protects counters from background neutrons.

The 4π neutron array TETRA was constructed at JINR, Dubna [12]. It consists of 80 counters filled by ^{3}He at 7 atm with a 1% admixture of CO_2. The cross section for the nuclear reaction

$$^3\mathrm{He} + \mathrm{n} \rightarrow {}^3\mathrm{H} + {}^1\mathrm{H} + 765\ \mathrm{keV} \quad (1)$$

is high in the thermal and low neutron energy range [13], so that polyethylene is used as a moderator to slow down the energetic neutrons to thermal energies by scattering. An admixture of many-atom gas such as CO_2 and some others attenuate the photoelectron emission [4]. Each counter is 50 cm in length and 32 mm in diameter. The small diameter of the central cavity provides almost 4π solid angle coverage. TETRA is one of the many neutron ^{3}He detectors built at JINR. Similar arrays were used in different experiments. For example, VASSILISSA neutron array [14–16] allows measurements of the neutron multiplicity and the half-life of heavy and superheavy nuclei in spontaneous fission [7]. SHIN array is used for low-background measurements to search for superheavy elements in natural samples by investigation of spontaneous fission events accompanied by high neutron multiplicity. FOBOS spectrometer and later miniFOBOS neutron array [17] allows the study of rare modes of spontaneous fission.

2.1. Design of the electronic system

The TETRA electronic channels are grouped into six clusters with 16 channels each (including one spare cluster). Fig. 2 shows a schematic diagram of the TETRA homemade electronics for each cluster. Each counter in a cluster has a built-in preamplifier. The operational high voltage is +1800 V applied to all counters via homemade distribution unit through an RC-filter. Charged particles produced in the active volume in the nuclear reaction of Eq. (1) trigger signals which feed a preamplifier. The gain of each amplifier channel is adjusted individually using an USB interface so that signals from all channels have the same amplitude. Neutron discrimination is obtained using low/high thresholds equal for all channels: all the events below the low threshold are rejected; whereas, events with amplitudes higher than the high threshold are recorded as neutron ones but with a special mark in a data buffer.

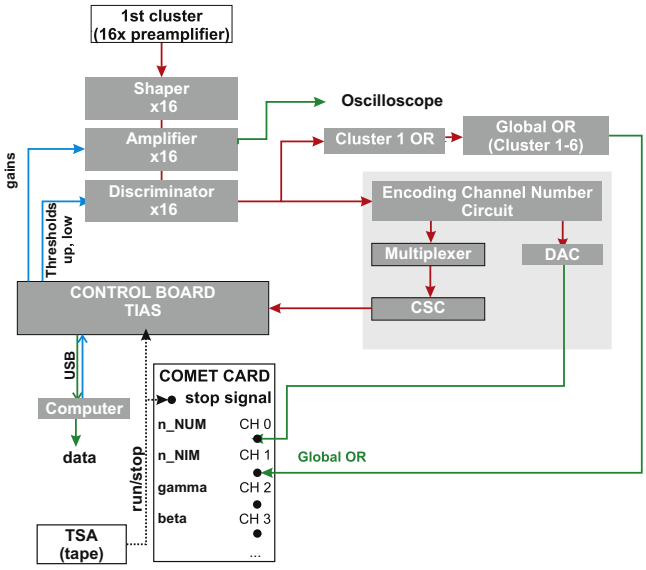

Fig. 2. Diagram for TETRA electronic system providing neutron data in a stand-alone mode and being coupled with COMET data acquisition system at BEDO. Synchronization is achieved thanks to the stop signal generated by the Tape Station Automate (TSA) (see text for details). For the sake of clarity only one TETRA cluster is shown.

Neutron data provided by TETRA can be stored simultaneously in two ways: by the integrated homemade acquisition system (TIAS) or by the triggerless data acquisition system COMET used presently at ALTO. A COMET card allows us to process data from up to 6 detectors determining the energy (coded on 15 bits) and time (coded on 47 bits) of signals from the detected radiation. Part of the processing is done in the card itself using the 32 bit 40 MHz digital signal processor [18].

Amplitude signals from the discriminator converted into logic ones are directly sent from TIAS to the COMET input channel "n-NIM" using a logic circuit "OR", see Fig. 2. Signals from the HPGe and the 4π β detectors, processed by typical electronic analog circuits, are sent to the next channels of the COMET card, see Fig. 2. Thus, neutrons, β and γ are counted simultaneously. β-γ or β-γ-neutron coincidences are built using the time stamp attributed by COMET. The counting rate is limited due to the occupation time of a COMET channel which is 10.3 μs.

To form a neutron counter identification number, signals from the discriminator are sent to the Encoding Channel Number Circuit (ECNC), see Fig. 2. The TIAS Digital to Amplitude Converter (DAC) generates a plateau voltage signal whose height is proportional to the identification number of the counter fired. Outputs of the DAC are recorded with time stamp attributed by COMET on its "n-NUM" channel. The occupation (coding + readout) time of the "n-NUM" channel being 25 μs, this identification information is only used for the on-line monitoring of the response of TETRA.

Alternatively, neutron data including a time stamp, the identification number of the counter fired and the high threshold mark can be stored by the TIAS running independently, coupled or in parallel with COMET. The TIAS allows the correct registration of neutron flashes of high multiplicity. The multiplexer which is a part of TIAS can hold up to 16 simultaneous neutron events, until they are processed. This allows the TIAS to correctly register high-multiplicity neutron events. The multiplexer transmits neutron events subsequently to the Control Board via a converter to the Serial Code (CSC). The time is defined by a counter with a 20-byte capture register. At overflow the time counter is reset to 0 with a stamp in the recorded data. Thus, whenever a counter is fired, the corresponding time stamp and the high threshold mark are stored by a computer via the USB interface.

A stop signal is triggered by the Tape Station Automate (TSA) in the beginning and in the end of each cycle, see Section 3, whenever the tape changes its state (motion/stopped). The stop signal prevents COMET and TIAS from taking data during tape motion and allows synchronization between them.

2.2. Pulse-height spectrum

A typical pulse-height spectrum measured from a neutron counter is presented in Fig. 3. If both reaction products, see Eq. (1), deposit all their energy in the active volume, the pulse-height spectrum at the output of a preamplifier of a ^{3}He counter has the form of an isolated peak. The low energy tail in the pulse-height spectrum corresponds to particles that have only partially lost their energy in the active volume. The low energy peak corresponds to ionization produced by γ-rays. High-amplitude events are largely due to alpha rays from the natural radioactivity of materials of the wall of a counter, and sparks. The pulse height spectra are used to tune the gain for each channel of the amplifier and the low/high discriminator thresholds.

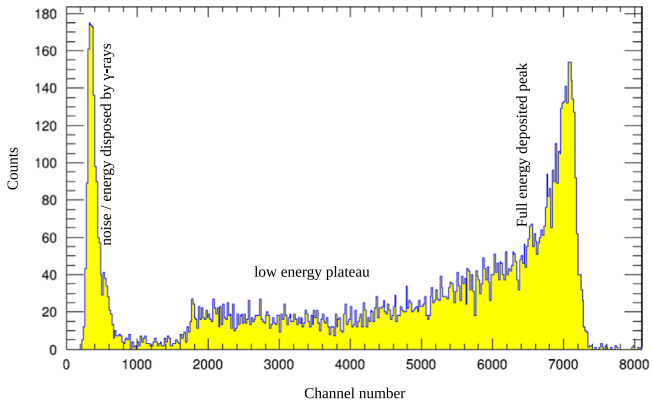

Fig. 3. A typical pulse height spectrum recorded for one counter with an AmBe source.

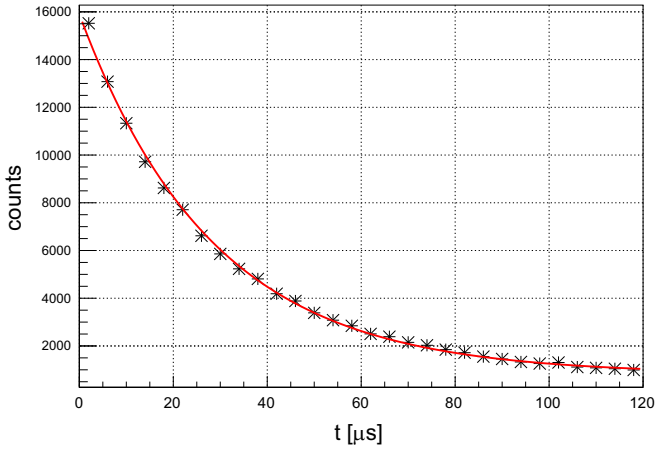

Fig. 4. Time difference between two consecutive neutrons emitted in spontaneous fission of ^{252}Cf. See text for details.

2.3. Neutron life-time in the detector

The neutron life-time in the detector τ is determined by moderation and diffusion times and can be estimated using the neutron time distribution relative to a start signal. A time difference distribution between two consecutive neutrons emitted in spontaneous fission of ^{252}Cf is presented in Fig. 4. The neutron life-time $\tau = 28.2(2)$ μs was obtained by fitting the experimental time difference distribution to a $(\exp(-t/\tau)+\text{const})$ function and is defined as the time difference in that half of the neutrons are detected.

2.4. Efficiency

The TETRA efficiency for single neutron detection was found by the method, proposed in [19], using a source whose neutron emission multiplicity distribution was known. This method was also used previously by our group [20]. Using a 8.0(4) kBq ^{252}Cf source placed at the center of the detector the multiplicity ratios were measured and compared to the calculated ones [21–23], as described in [19] to derive the efficiency $\epsilon_0 = 53(2)\%$. The obvious advantage of the method is independence from the initial measurements of neutron activity of a source provided in a source certificate. Furthermore, the method provides a consistent test since the measured multiplicity ratios must satisfy the calculated multiplicity ratios unless there is an electronic problem or a mistake in the analysis. The method can be applied for any spontaneous fission neutron sources whose multiplicity distribution is known. The efficiency of a single neutron event measured by the method described above is valid only for a source with an energy spectrum similar to the one of ^{252}Cf [24]. Therefore, to determine the effective neutron detection efficiency associated to the effective response of the detector to the neutron energy spectrum an alternative method based on β-neutron-γ coincidence should be used. An illustration of this method is provided by the absolute measurement of P_{1n}-value of ^{82}Ga in Section 3.

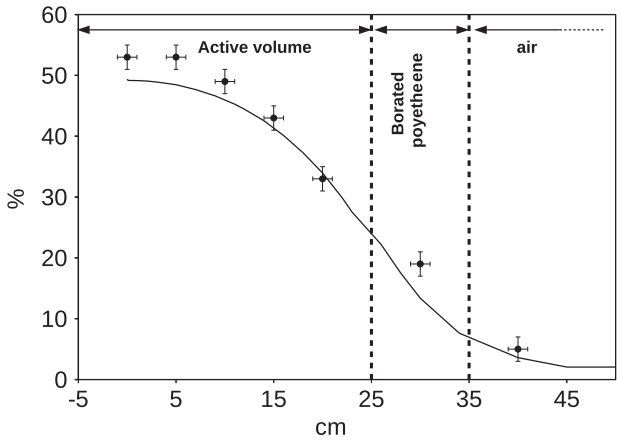

Fig. 5. Calculated (line) and measured (symbols) efficiency of TETRA as a function of distance along the axis for moving the ^{252}Cf source from the center of the detector.

2.5. MCNP simulations for TETRA

To optimize the installation of TETRA on the BEDO tape station a validated computer model of TETRA was highly needed. This model was created using the MCNP code (Monte Carlo N Particle transport) [25] (version MCNP5 RSICC 1.40) and is reported in [26]. The efficiency of the TETRA array for a ^{252}Cf source moving inside the detector on the beam axis from its center with zero coordinate was measured by the method described above and calculated by the MCNP model, see Fig. 5. Within the 1–2 cm from the center the efficiency is almost flat but gradually decreases with increasing distance. As can be seen, the calculations regularly underestimate the experimental points. Such a deviation originates from allowances of the modeling: neglecting minor materials, uncertainty in densities and geometrical dimensions of parts of the detector. The comparison of the measured and the calculated distributions via χ^2-criteria shows that the model can be trusted within 9% of absolute error bars. This uncertainty level was accepted to prove the optimum ^{3}He gas pressure, the choice of moderation material and the anti-background shielding [26]. The calculated efficiency of TETRA as a function of neutron energy is almost constant up to 0.8 MeV and as presented in Fig. 6.

3. Commissioning experiment

3.1. Experimental procedure

The commissioning of TETRA was performed during an experiment at ALTO aiming at studying the decays of $^{82\text{-}84}$Ga. The half-life and the probability of β-delayed neutron emission for ^{82}Ga were already measured several times and can be considered as well established [27–32]. For that reason ^{82}Ga was chosen as the test/reference case presented here while results on ^{83,84}Ga obtained, for consistency, in exactly the same experimental conditions, will be communicated in a separate article. Beams of neutron rich Ga isotopes were obtained from the fission of ^{238}U

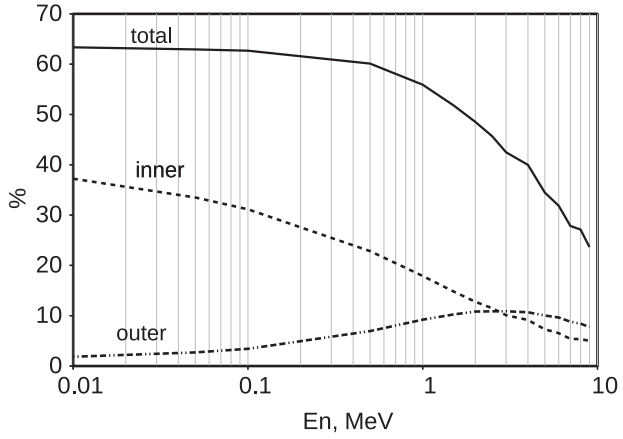

Fig. 6. *Solid line*: total calculated neutron detection efficiency of the full setup; *dashed line*: calculated efficiency of the inner ring #1; *dotted-dashed line*: calculated efficiency of the outer ring #4.

contained in UC_x pellets (≈ 60 g of ^{238}U) placed into a Ta oven exposed to the 50 MeV ($\lesssim 10$ μA) primary electron beam. The oven was heated up to ≈ 2000 °C to fasten the release of the fission products towards the transfer tube. Ga atoms were selectively ionized with the Resonant Ionization Laser Ion Source (RILIS) using a two-step ionization scheme [34]. The ionization efficiency was measured from a comparison between the laser-on and laser-off intensities and did not exceed 5% on the average, a value somewhat lower than the one obtained during the previous laser run reported in [35]. After extraction at 30 keV energy, the beam was sent towards the on-line isotope separator PARRNe then transported to the BEDO station (see [8] for more details). In these experimental conditions, the mass-analyzed effective ^{82}Ga beam intensity at the collection point was determined to be 1290(60) pps as will be shown later.

As explained previously, the ^{82}Ga beam was collected onto the mylar tape at the center of the detection array. The radioactive sources thus created were cyclically transported out of the setup to avoid accumulation of the longer lived daughter activities. A short beam-off counting time $T_{bg} = 100$ ms was set before each beam collection to estimate the evolution of the background during the experiment and to monitor possible activity built-in off the tape. After ion collection during $T_{beam} = 2$ s the beam was deflected, and the tape was moved for 2 m to transport the source outside the detection array. The resulting β and neutron activity curves, accumulated over 1700 cycles are presented in Fig. 7. The cumulated neutron counts within T_{bg} amount to an average neutron background limited to ≈ 10 n/s in order of magnitude. It certainly originates from the β^-n activities accumulated in the mass separator and cosmic rays. The background was reduced both by improving the shielding of the separator adding locally a three layer (high density polyethylene–Cd–Pb) sandwich to the concrete wall (see Fig. 2 in Ref. [8]) surrounding it and by shielding TETRA itself as described earlier. The β background counting rate (≈ 30 β/s) was due to slight fluctuations of the beam alignment which led to beam accumulation inside the detection system but off the tape. To minimize this effect the BEDO tape station was equipped at the origin with two pairs of horizontal and vertical slits before the entrance cube (see Fig. 3 in Ref. [8]).

All the γ activities recorded for a mass 82 setting of the separator could be identified and no isobaric contaminants were observed within our detection limits, see Fig. 8. We note that, in a laser ionization production mode at ALTO, Ga is its own surface-ionized contaminant and in fact the only possible one at $A=82$, owing to the inherent selectivity of the dominant production process which is photofission (no neutron deficient isobars). In

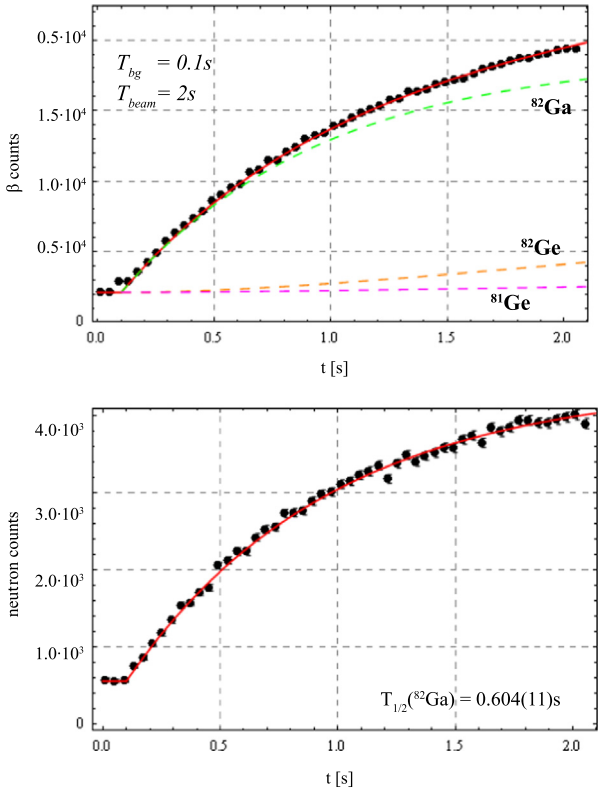

Fig. 7. β (top) and neutron (bottom) activity curves from the collection of the ^{82}Ga beam onto the tape. The curves were accumulated over 1700 tape cycles. Different contributors to the total β activity are shown by colored dashed lines (see text for the details on the way they were obtained). The neutron activity can be attributed solely to $^{82}Ga \xrightarrow{\beta-n} {}^{81}Ge$ decay (see text). The grow-in curve is then characterized by the half-life of the ^{82}Ga precursor. The fitted half-life for ^{82}Ga is 0.604(11) s (red line). (For interpretation of the references to color in this figure caption, the reader is referred to the web version of this paper.)

addition, no evidence for contamination from surface ionized ^{82}Ge has been found in the analysis of the grow-in activity curves, as will be seen later. This is expected: such a contamination is indeed unlikely due to the high ionization potential of Ge.

The decay chains over three generations following the decay of ^{82}Ga are shown in Fig. 9 for the sake of convenience. In Fig. 8, a comparison between the direct (ungated), the β-gated and the β-neutron gated γ-spectra is presented. As can be seen from this figure, while γ-rays associated to transitions in the daughter nuclei (^{81,82}Ge, ^{81,82}As, ^{82}Se) are present in the β-gated spectrum, the doubly β-neutron gated spectrum only contains peaks characterizing the $^{82}Ga \xrightarrow{\beta-n} {}^{81}Ge$ decay. Only three γ-transitions were attributed to the β-n channel of the ^{82}Ga decay [37,38] prior to our measurement. We can unambiguously add four new γ-rays to this channel at 562.8(4), 828.3(4), 936.6(4) and 1286.4(5) keV, see Table 1. These energies are compatible with those of transitions in ^{81}Ge already known to be fed in the ^{81}Ga decay [38] and we propose to attribute these γ-rays to them.

3.2. Efficiency determination

The efficiency of TETRA for prompt neutrons of spontaneous fission of ^{252}Cf was measured as described in Section 2.4 to be 53 (2)%. However this efficiency is valid only for a neutron source with a neutron energy spectrum similar to the one of ^{252}Cf. The β-delayed neutron energy spectrum for ^{82}Ga is significantly different [41]. We propose a simple method to determine an "effective" neutron efficiency $\overline{\epsilon}_n$ relying on the coincidence data between the three (β, γ, neutron) detectors composing the system. To this end

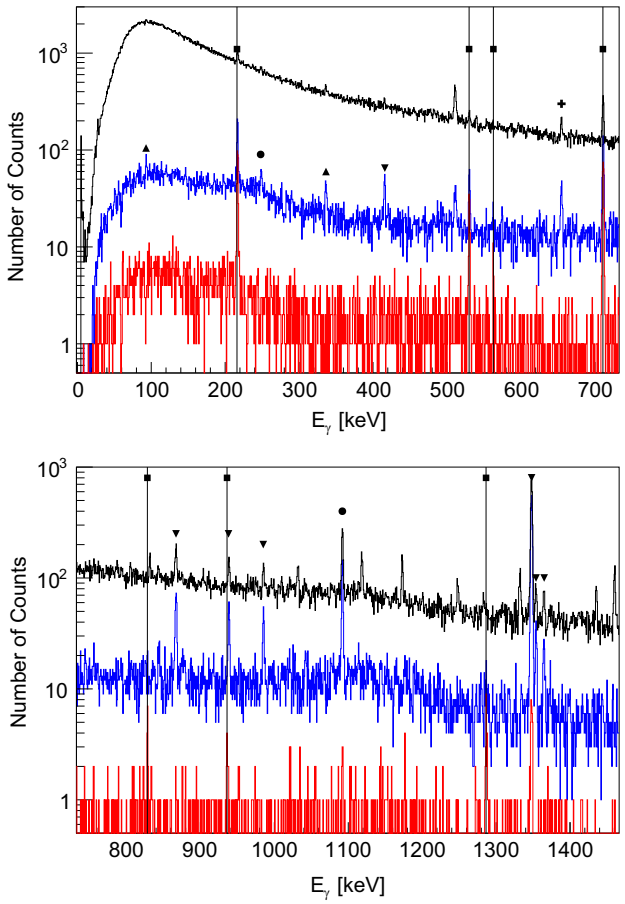

Fig. 8. Experimental direct (black line), β-gated (blue line) and β-neutron gated (red line) γ spectra obtained at $A=82$. ▾ : ^{82}Ga$\xrightarrow{\beta^-}$^{82}Ge, ● : ^{82}Ge$\xrightarrow{\beta^-}$^{82}As, ✚: ^{82}As$\xrightarrow{\beta^-}$^{82}Se, ■ : ^{82}Ga$\xrightarrow{\beta^-n}$^{81}Ge, ▴ : ^{81}Ge$\xrightarrow{\beta^-}$^{81}As. (For interpretation of the references to color in this figure caption, the reader is referred to the web version of this paper.)

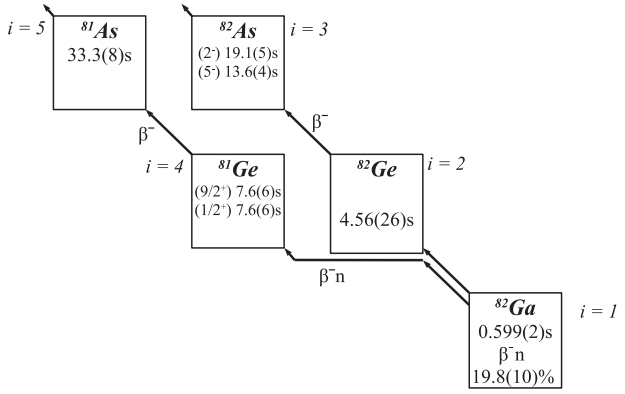

Fig. 9. Decay scheme of neutron-rich ^{82}Ga isotope. Half-lifes and the P_{1n}-value are taken from the ENSDF database [36].

we use the ratio between the doubly β-n gated and singly β gated γ-spectra of background subtracted peak areas for a given γ-ray i emitted in the β-n channel as an estimate of the neutron detection efficiency $\epsilon_n^i = S_{\gamma\beta n}^i / S_{\gamma\beta}^i$. This could be done for the three strongest peaks observed (216, 530 and 711 keV) and the results are reported in Table 1. The fluctuations between the different ϵ_n^i values are due to variations of the neutron efficiency with the neutron energy and are used as an estimate of the systematic error. The weighed average of the ϵ_n^i values is then taken as $\overline{\epsilon}_n$. This quantity is an effective neutron detection efficiency in the sense that it

Table 1
Energies and intensities of the γ-ray transitions from the decays of ^{82}Ga. Intensities are measured relative to the 711 keV transition (or to the 1348 keV transition if marked by *). In the 5th column (Spec.) are indicated the γ-spectra of Fig. 8 which were used to determine the different quantities, labeled γ for the direct, γβ for the singly β-gated and γβn for doubly β-neutron gated γ-spectra. ϵ_n^i and ϵ_β^i are the neutron and β detection efficiencies, respectively, as defined in the text. Level energies are from Ref. [37–40].

Decay	E_γ [keV]	E_{level} [keV]	I^{rel} [%]	Spec.	ϵ_β^i [%] $S_{\gamma\beta}^i/S_\gamma^i$	ϵ_n^i [%] $S_{\gamma\beta n}^i/S_{\gamma\beta}^i$
^{82}Ga$\xrightarrow{\beta^-n}$^{81}Ge	216.9(3)	895.6	33(4)	γβ	52(8)	
			40(20)	γβ n		60 (6)
^{82}Ga$\xrightarrow{\beta^-n}$^{81}Ge	530.5(4)	1241.3	24(4)	γβ		
			27(14)	γβ n		66(9)
^{82}Ga$\xrightarrow{\beta^-n}$^{81}Ge	711.4(4)	711.1	17(1)*	γβ	52(4)	
			100(48)	γβ n		64(4)
^{82}Ga$\xrightarrow{\beta^-n}$^{81}Ge	562.8(4)	1241.3	6(2)	γβ n		
^{82}Ga$\xrightarrow{\beta^-n}$^{81}Ge	828.3(4)	1724.0	6(3)	γβ n		
^{82}Ga$\xrightarrow{\beta^-}$^{82}Ge	867.2(4)	2286.36	8(2)*	γβ	64(7)	
^{82}Ga$\xrightarrow{\beta^-n}$^{81}Ge	936.6(4)	1832.2	4(2)	γβ n		
^{82}Ga$\xrightarrow{\beta^-}$^{82}Ge	985.5(4)	2333.1	6(2)*	γβ	57(10)	
^{82}Ga$\xrightarrow{\beta^-n}$^{81}Ge	1286.4(5)	1286.4	15(6)	γβ n		
^{82}Ga$\xrightarrow{\beta^-}$^{82}Ge	1348.1(5)	1348.4	100(3)*	γβ	69(2)	
^{82}Ga$\xrightarrow{\beta^-}$^{82}Ge	1092.4(5)	1092.0	20(2)*	γβ	64(5)	
^{82}Ga$\xrightarrow{\beta^-}$^{82}Ge	1909.4(5)	3257.41	10(2)*	γβ	64(8)	

takes into account the neutron energy distribution effect in an effective way and will necessarily vary from one isotope to the other. The result for this ^{82}Ga measurement is $\overline{\epsilon}_n = 63(6)\%$. The β efficiency was obtained with the same method, see Table 1, and we obtain $\overline{\epsilon}_\beta = 63(4)\%$.

3.3. P_{1n} extraction procedure

The P_{1n} value of a β-delayed neutron precursor is the ratio between the number of neutrons emitted after β-decay and the total number of β decays. There are different methods to experimentally determine P_{1n} values. These approaches differ in the ways mother, daughter and granddaughter nuclei are counted [42,43]. In the present experiments β and neutron activities were recorded simultaneously (see Fig. 7). All neutrons detected for $A=82$ were attributed either to the background or to the ^{82}Ga β-n decay: β-delayed neutron emission is indeed energetically not possible for the other isotopes with higher Z in the $A=82$ isobaric chain. The fit of the growth pattern of the recorded neutron activity (Fig. 7), leads to a ^{82}Ga half-life value of 0.604(11) s where the uncertainty is the uncertainty from the fit. As can be seen in Fig. 10, this value is compatible with those from previous experiments. It shows that if beam fluctuations occurred they had no sizable effect on the final shape of the accumulated grow-in curves. We will hence assume in the following a constant *average* beam rate.

The decay of a radioactive source created by the collection of the ^{82}Ga beam onto the tape is characterized by the decay constants λ_i ($i=1\ldots5$) of the parent [^{82}Ga ($i=1$)], daughters [^{81}Ge ($i=4$), ^{82}Ge ($i=2$)] and granddaughter nuclei [^{81}As ($i=5$), ^{82}As ($i=3$)] as well as by the P_{1n} value of ^{82}Ga as illustrated in Fig. 9. If we note $N_i(t)$ the population of each nucleus $i=1\ldots5$ onto the tape at a given time t, the total decayed population A^{tot} at the end of the measurement time T_{meas} is

$$A^{tot} = A_\beta^{tot} = \sum_{i=1}^{5} \int_{T_{bg}}^{T_{meas}} \lambda_i \cdot N_i(t)\, dt. \qquad (2)$$

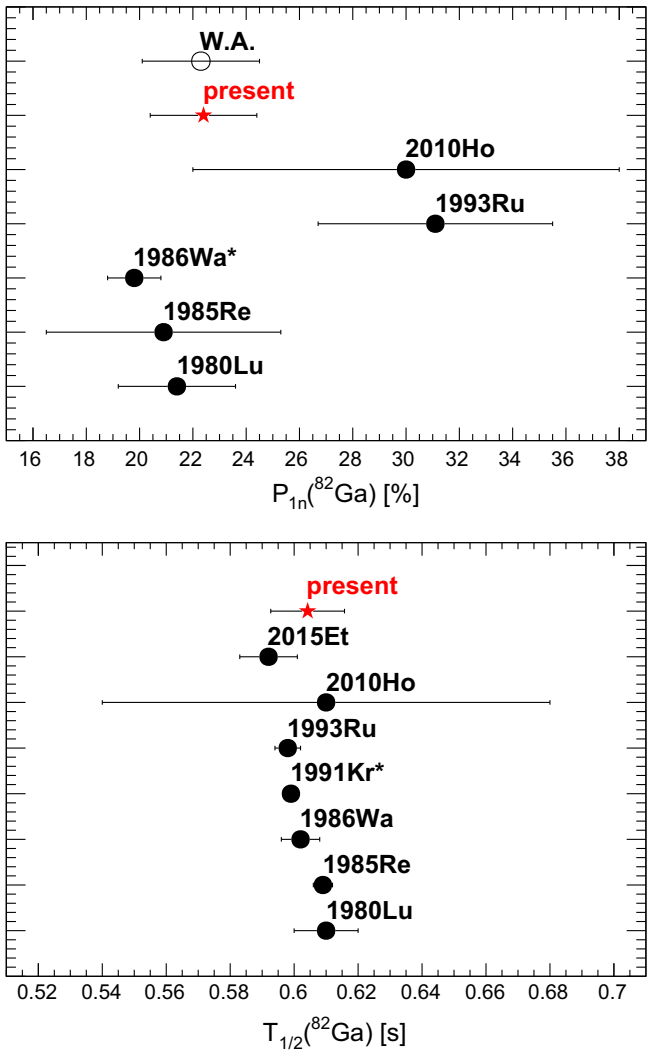

Fig. 10. Presently measured P_{1n}(top) and $T_{1/2}$(bottom) determined by recorded neutron activity for ^{82}Ga are marked by red stars and compared to other works: 1980Lu – [27], 1985Re – [28], 1986Wa – [29]*, 1991Kr – [30]*, 1993Ru – [31], 2010Ho – [32], 2015Et – [8]. (*) – values currently adopted by the ENSDF evaluator; "W.A." refers to the weighted average from the evaluation in Ref. [31] and the compilation of Ref. [33]. (For interpretation of the references to color in this figure caption, the reader is referred to the web version of this paper.)

Since all the nuclei in Fig. 9 decay 100% by β-decay, the total number of β, A_β^{tot}, emitted during $T_{coll} = T_{meas} - T_{bg}$, is $A_\beta^{tot} = A^{tot}$. Therefore, the collected β and neutron statistics, N_β^{stat}, N_n^{stat}, can be described by the following equation:

$$\begin{cases} N_\beta^{stat} = (N_\beta^{exp} - N_\beta^{bg})\frac{1}{\overline{\epsilon}_\beta} = \sum_{i=1}^{5} \int_{T_{bg}}^{T_{meas}} \lambda_i \cdot N_i(t)\, dt, \\ N_n^{stat} = (N_n^{exp} - N_n^{bg})\frac{1}{\overline{\epsilon}_n} = P_{1n} \cdot \int_{T_{bg}}^{T_{meas}} \lambda_1 \cdot N_1(t)\, dt, \end{cases} \quad (3)$$

where N_β^{exp}, $N_n{}^{exp}$ are total numbers of β and neutrons detected; N_β^{bg} and $N_n{}^{bg}$ are the total number of background events; $\overline{\epsilon}_\beta$ and $\overline{\epsilon}_n$ are the β and neutron detection effective efficiencies, respectively, determined as described above. Following our notation the ^{82}Ga beam rate, ϕ (s^{-1}), appears explicitly in the expression of $N_1(t)$ *via*

$$dN_1(t)/dt = -\lambda_1 \cdot N_1(t) + \phi. \quad (4)$$

By writing the system of Eqs. (3) and (4) we make the following assumptions:

(i) the background level evaluated during $T_{bg} = 0.1$ s before collecting the beam remains constant during the subsequent $T_{coll} = 2$ s of beam collection;

and, as already discussed previously:

(ii) the beam rate is considered as a constant average ϕ;
(iii) the only beam feeding contribution is to the ^{82}Ga population.

These hypotheses will be further tested in a second step (see below).

The first step consists in solving the system of Eqs. (3) and (4) to obtain P_{1n} and ϕ taking λ_i ($i = 2\ldots5$) from the literature and λ_1 as previously determined from our neutron activity curve. To determine the uncertainty on these values we took into consideration the uncertainties on λ_i ($i = 1\ldots5$) (in the case $i = 2\ldots5$ from the evaluation) and the uncertainty on the β and neutron counts and associated backgrounds which take into account the systematic errors on the detection efficiencies as discussed above. To do so, the system is first solved to obtain the central values P_{1n}^0, ϕ^0 with the central values of the parameters. Then it is solved for each of the parameters λ_i, N_β^{stat} and N_n^{stat} varied within their error bars to obtain a set of solutions $P_{1n}^{\lambda_i}, \phi^{\lambda_i}$ ($i = 1\ldots5$), $P_{1n}^{N_\beta^{stat}}, \phi^{N_\beta^{stat}}, P_{1n}^{N_n^{stat}}, \phi^{N_n^{stat}}$. The final uncertainties $\sigma(P_{1n})$ and $\sigma(\phi)$ were obtained simultaneously as a root square from the sum of quadratic deviations around the mean P_{1n}^0, ϕ^0 values:

$$\sigma(P_{1n}) = \sqrt{\sum_{i=1}^{5} (P_{1n}^0 - P_{1n}^{\lambda_i})^2 + (P_{1n}^0 - P_{1n}^{N_\beta^{stat}})^2 + (P_{1n}^0 - P_{1n}^{N_n^{stat}})^2} \quad (5)$$

and similarly for $\sigma(\phi)$. This procedure leads to P_{1n} (^{82}Ga)=22.2 (20)% and $\phi = 1290(60)\ s^{-1}$. As can be seen in Fig. 10 the so obtained P_{1n} value is in very good agreement with the weighted average of the values obtained in previous experiments. The final error on P_{1n} is dominated by the N_β^{stat} and N_n^{stat} terms in Eq. (5) which contain the systematic errors on the efficiencies.

To further test hypotheses (i)–(iii) above we have verified, in a second step, that the $T_{1/2}$, ϕ, P_{1n} values so obtained for ^{82}Ga were consistent with the observed pattern of the β activity curve by carrying out a fit of this curve. The fitting functions were the analytical expressions of the activities $A_i(t) = \lambda_i \cdot N_i(t)$ ($i = 1\ldots5$) with 7 free parameters λ_i ($i = 1\ldots5$), ϕ and P_{1n}. The initial values of the parameters were taken to be: λ_1(^{82}Ga) determined from our neutron activity curve, λ_i ($i = 2\ldots5$) from the literature, ϕ and P_{1n} as determined above. The parameters were allowed to vary within their associated uncertainties. The resulting β-activity curves are plotted in Fig. 7. We note that varying λ_i ($i = 1\ldots5$), ϕ, P_{1n} parameters within their the uncertainty had a negligible effect on the fit. The almost perfect reproduction of the measured β-activity curve shows that the contributions from potential increasing background, beam rate variations or ^{82}Ge beam component, should they exist, are negligible.

The fact that the $T_{1/2}$ (from the neutron curve) and P_{1n} values obtained for ^{82}Ga are in good agreement with those available in the literature, as well as the consistent reproduction of the cumulated β curve can be considered as a validation of the chosen method. It proves in particular the capacity to measure P_{1n} values with a reasonable accuracy with the TETRA ^{3}He neutron counter even in cases of unknown neutron energy spectra. This is mainly due to the simultaneous use of a β and a high resolution γ detectors which allow determining the global response of the detector.

4. Summary

The 4π high efficiency neutron detector TETRA built at JINR, Dubna has been modified enabling measurements of β-decay properties of neutron-rich nuclei produced at the recently inaugurated ISOL facility ALTO (Orsay). The unique design of the detection system was imposed by the requirement to have a constant neutron efficiency up to 0.8 MeV and the necessity to record simultaneously β, γ and neutron activities from a radioactive source accumulated inside the detection system. For optimizing the coupling of TETRA with the recently built BEDO decay station, a series of MCNP simulations was performed. A determination of the TETRA efficiency was achieved using a robust method based on multiplicity distribution of prompt neutrons emitted from a ^{252}Cf spontaneous fission source. It is consistent with the results obtained from MCNP simulations demonstrating that the neutron detection process in this new configuration is well understood. The on-line performances of the TETRA array coupled to the BEDO decay station were further investigated. A laser-ionized beam of ^{82}Ga, with well established $T_{1/2}$ and P_{1n}, was chosen for that purpose. By using the 4π β and TETRA effective efficiencies determined from β-neutron gated γ spectra analysis we obtained $T_{1/2}$ and P_{1n} values for ^{82}Ga in remarkable agreement with those available in the literature.

Furthermore, the TETRA integrated data acquisition system is designed to make TETRA a tool of choice for detection of high multiplicity neutron events. This feature will be important for the upcoming experiments with beams of neutron rich-nuclei for which larger Q_β values result in higher multi-neutron emission probability. We have also demonstrated the ability of TETRA to be used as neutron trigger for β-decay γ-spectroscopy despite the inherently slow neutron registration process.

Acknowledgements

The authors wish to acknowledge support from the bilateral agreement JINR-CNRS and the TETRA collaboration. Also we would wish to acknowledge the support of the Russian Foundation for Basic Research, Grant no. 14-02-91053CNRSa and of the Projet International de Coopération Scientifique (PICS) between CNRS/IN2P3 and JINR. We thank the technical staff of the Tandem/ALTO facility for their assistance with the experiments and for providing excellent quality radioactive beams. The use of one Ge detector from the French-UK IN2P3-STFC Gamma Loan Pool is acknowledged.

References

[1] Y. Blumenfeld, T. Nilsson, P. Van Duppen, Physica Scripta T152 (2013) 014023 (Nobel Symposium: Physics with Radioactive Beams, vol. 152, Göteborg, Sweden, June 2012, pp. 11–15).
[2] K.L. Kratz, F.K. Thielemann, W. Willebrandt, et al., Journal of Physics G: Nuclear Physics 14 (1988) S331.
[3] M. Arnould, S. Goriely, K. Takahashi, Physics Reports 450 (2007) 97.
[4] T. Crane, M. Baker, Passive nondestructive assay of nuclear materials, in: D. Reilly et al. (Eds.), LA-UR-90-732 Neutron Detectors, Los Alamos National Laboratory, Los Alamos, 1991 (Chapter 13).
[5] J. Pereira, P. Hosmer, G. Lorusso, et al., Nuclear Instruments and Methods A 618 (2010) 275.
[6] R. Caballero-Folch, C. Domingo-Pardo, G. Cortès, et al., Nuclear Data Sheets 120 (2014) 81.
[7] D. Testov, Ch. Briançon, S. Dmitriev, et al., Journal of Physics and Atomic Nuclei 72 (2009) 1.
[8] A. Etilé, D. Verney, N.N. Arsenyev, et al., Physical Review C 91 (2015) 064317.
[9] F. Azaiez, S. Essabaa, F. Ibrahim, D. Verney, Nuclear Physics News 23 (2013) 2.
[10] S. Essabaa, et al., Nuclear Instruments and Methods B 317 (2013) 218.
[11] C. Beausang, S. Forbes, P. Fallon, et al., Nuclear Instruments and Methods A 313 (1992) 37.
[12] G. Ter-Akopian, A. Popeko, E. Sokol, et al., Nuclear Instruments and Methods A 190 (1981) 119.
[13] Korea Atomic Energy Research Institute Nuclear Data Evaluation Laboratory, November 2007 ⟨http://www.atom.kaeri.re.kr/⟩.
[14] A. Yeremin, A. Belozerov, M. Chelnokov, et al., Nuclear Instruments and Methods A 539 (2005) 441.
[15] A. Svirikhin, Ch. Briançon, S. Dmitriev, et al., in: AIP Conference Proceedings, vol. 1175, 2009, p. 297.
[16] A. Svirikhin, A. Isaev, A. Yeremin, et al., Instruments and Experimental Techniques 54 (2011) 644.
[17] Y. Pyatkov, D. Kamanin, W. Oertzen, et al., European Physics Journal A 48 (2012) 1.
[18] J. Le Bris, R. Sellem, J. Artiges, et al., Internal Report IPNO 06-003, 2006, 06-03.
[19] M. Dakowski, Y. Lazarev, V. Turchin, et al., Nuclear Instruments and Methods 113 (1973) 195.
[20] E. Sokol, V. Smirnov, S. Lukyanov, Nuclear Instruments and Methods A 400 (1997) 96.
[21] A.S. Vorobyev, V.N. Dushin, F.-J. Hambsch, in: AIP Conference Proceedings vol. 769, 2005, p. 613.
[22] R.R. Spencer, R. Gwin, R. Ingle, Nuclear Science and Engineering 80 (1982) 603.
[23] J.W. Boldeman, M.G. Hines, Nuclear Science and Engineering 91 (1985) 114.
[24] M.V. Blinov, G.S. Boykov, V.A. Vitenko, Nuclear Data for Science and Technology 479 (1983).
[25] LA-UR-03-1987, MCNP A General Monte Carlo N-Particle Transport Code, Version 5, 2003.
[26] D. Testov, E. Kuznetcova, J. Wilson, Journals of Instrumentation 10 (2015) P09011.
[27] E. Lund, P. Hoff, K. Aleklett, et al., Zeitschrift fr Physik A 294 (1980) 233.
[28] P. Reeder, R. Warner, M. Edminston, R. Gill, A. Pietrowski, in: Proceedings of the American Society of Nuclear Chemistry Meeting, Chicago, 1985, p. 171.
[29] R.A. Warner, P.L. Reeder, Radiation Effects 94 (1986) 27.
[30] K.-L. Kratz, H. Gabelmann, P. Möller, et al., Zeitschrift fr Physik 340 (1991) 419.
[31] G. Rudstam, K. Aleklett, L. Sihver, Atomic Data and Nuclear Data Tables 53 (1993) 1.
[32] P. Hosmer, H. Schatz, A. Aprahamian, et al., Physical Review C 82 (2010) 025806.
[33] B. Pfeiffer, K.-L. Kratz, P. Möller, Progress in Nuclear Energy 41 (2002) 39.
[34] R. Li, J. Lassen, A. Teigelhöfer, et al., Nuclear Instruments and Methods B 308 (2013) 74.
[35] K. Kolos, D. Verney, F. Ibrahim, et al., Physical Review C 88 (2013) 047301.
[36] (08/2013) ⟨http://www.nndc.bnl.gov/ensdf/⟩.
[37] P. Hoff, NFL-22 1980.
[38] C.M. Baglin, Nuclear Data Sheets 109 (2008) 2257.
[39] P. Hoff, B. Fogelberg, Nuclear Physics A 368 (1981) 210.
[40] J.A. Winger, et al., Physical Review C 81 (2010) 044303.
[41] ⟨http://www.nndc.bnl.gov/sigma/⟩.
[42] D. Abriola, B. Singh, I. Dillmann, Beta-delayed Neutron Emission Evaluation, IAEA(NDS)-0599, 1999.
[43] I. Dillmann, P. Dimitriou, B. Singh, Beta-Delayed Neutron Emission Evaluation, IAEA(NDS)-0643, 2014.